Dynamic Walking Conference 2012
May 21-24, 2012 Pensacola beach, Florida, USA

Indicators for Emergence of Double-limb Support in Passive Dynamic Walking

Fumihiko Asano

School of Information Science, Japan Advanced Institute of Science and Technology (JAIST)

1. Motivation and State of the Art

The effects of double-limb support (DLS) motion must play important roles in stable dynamic walking. The mechanism of DLS, however, has not been investigated in detail in the field of limit cycle walking because the stance-leg exchange is generally modeled on the assumption of inelastic collision; the rear leg leaves the ground just after the touchdown of the fore leg [1].

Based on the observations, the authors have investigated the potentiality of the emergence of DLS motion in passive cycle walking (PDW).We confirmed that a viscoelastic-legged rimless wheel (VRW) shown in Fig. 1 emerges the measurable period of DLS through numerical simulations and experiments [2]. The purposes of this study are to identify the conditions for the emergence of DLS motion in PDWand to specify the computational procedure for transition to DLS.

2. Passive Telescopic-legged Rimless Wheel

Fig. 1 shows our experimental VRW (left) and the ideal model (right). This consists of eight identical telescopic-leg frames with viscoelasticity. Let c [N·s/m] be the viscosity coefficient and k [N/m] be the elastic coefficient. Let

$$\boldsymbol{q} = \begin{bmatrix} x & z & \theta & L_1 & L_2 \end{bmatrix}^{\mathrm{T}}$$

be the generalized coordinate vector. The robot equation of motion then becomes

$$\boldsymbol{M}(\boldsymbol{q})\ddot{\boldsymbol{q}} + \boldsymbol{h}(\boldsymbol{q},\dot{\boldsymbol{q}},\phi) = \boldsymbol{J}(\boldsymbol{q})^{\mathrm{T}}\boldsymbol{\lambda}, \quad \boldsymbol{J}(\boldsymbol{q})\dot{\boldsymbol{q}} = \boldsymbol{0}$$

where the Jacobian matrix, $\boldsymbol{J}(\boldsymbol{q})$, is selected according to the contact conditions. The second equation represents the holonomic constraint condition. In the period of DLS, the following two conditions hold.

- The end-point of Leg 1 (the fore support leg in the model of Fig. 1) contacts the floor without slipping. (⇒ *Constraint 1*)
- The end-point of Leg 2 (the rear support leg in the model of Fig. 1) contacts the floor without slipping. (⇒ *Constraint 2*)

The holonomic constraint force can be divided in to

$$\boldsymbol{J}_{\mathrm{DLS}}(\boldsymbol{q})^{\mathrm{T}}\boldsymbol{\lambda} = \begin{bmatrix} \boldsymbol{J}_1^{\mathrm{T}} & \boldsymbol{J}_2^{\mathrm{T}} & \boldsymbol{J}_3(\boldsymbol{q})^{\mathrm{T}} & \boldsymbol{J}_4(\boldsymbol{q})^{\mathrm{T}} \end{bmatrix} \begin{bmatrix} \lambda_1 \\ \lambda_2 \\ \lambda_3 \\ \lambda_4 \end{bmatrix} = \boldsymbol{J}_1^{\mathrm{T}}\lambda_1 + \boldsymbol{J}_2^{\mathrm{T}}\lambda_2 + \boldsymbol{J}_3(\boldsymbol{q})^{\mathrm{T}}\lambda_3 + \boldsymbol{J}_4(\boldsymbol{q})^{\mathrm{T}}\lambda_4.$$

Constraint 1 Constraint 2

These terms (ground reaction forces of Leg 2) becomes zero after the motion transitions to SLS.

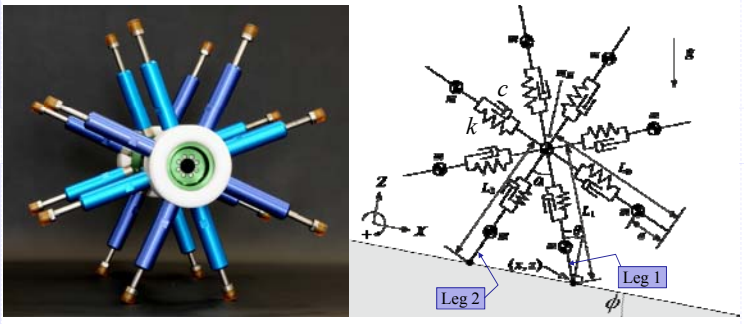

Figure 1: Experimental viscoelastic-legged rimless wheel (left) and its ideal model (right)

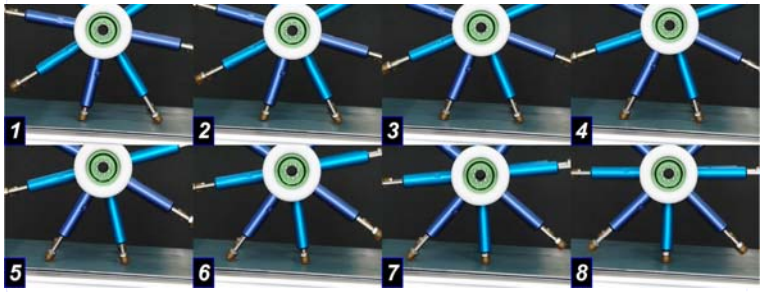

Figure 2: Snapshots of double-limb support motion in passive dynamic walking

3. Our Approach

3.1 Computational procedure for velocity just after impact

The equations for inelastic collision of Leg 1 with the ground becomes

$$\boldsymbol{M}(\boldsymbol{q}^{\dagger})\dot{\boldsymbol{q}}^{+} = \boldsymbol{M}(\boldsymbol{q}^{\dagger})\dot{\boldsymbol{q}}^{\dagger} + \boldsymbol{J}_I(\boldsymbol{q}^{\dagger})^{\mathrm{T}}\boldsymbol{\lambda}_I, \quad \boldsymbol{J}_I(\boldsymbol{q}^{\dagger})\dot{\boldsymbol{q}}^{+} = \boldsymbol{0}$$

and the Jacobian matrix is selected in accordance with the following algorithm.

1. We set $\boldsymbol{J}_I(\boldsymbol{q}) = \boldsymbol{J}_{\mathrm{DLS}}(\boldsymbol{q}) \in R^{4\times 5}$ and compute $\boldsymbol{\lambda}_I(\boldsymbol{q}) = \begin{bmatrix} \lambda_{I1} & \lambda_{I2} & \lambda_{I3} & \lambda_{I4} \end{bmatrix}^{\mathrm{T}}$.
2. $\lambda_{I2} \geq 0$ and $\lambda_{I4} \geq 0$ must hold to transition to DLS. It is obvious, however, that $\lambda_{I2} > 0$ always holds. Therefore we should check the sign of λ_{I4} only.
3. If $\lambda_{I4} < 0$, DLS motion does not emerge. We then compute $\dot{\boldsymbol{q}}^{+}$ by setting $\boldsymbol{J}(\boldsymbol{q}^{\dagger}) = \boldsymbol{J}_{\mathrm{SLS}}$.
4. If $\lambda_{I4} \geq 0$, the motion then transitions to DLS and we compute $\dot{\boldsymbol{q}}^{+}$ by setting $\boldsymbol{J}(\boldsymbol{q}^{\dagger}) = \boldsymbol{J}_{\mathrm{DLS}}(\boldsymbol{q}^{\dagger})$.

3.2 Computational procedure for acceleration just after impact

1. If $\lambda_{I4} \geq 0$, the motion is determined to transition to DLS. The equations of motion just after impact are then specified as
$$\boldsymbol{M}(\boldsymbol{q}^{\dagger})\ddot{\boldsymbol{q}}^{+} + \boldsymbol{h}(\boldsymbol{q}^{\dagger},\dot{\boldsymbol{q}}^{+},\phi) = \boldsymbol{J}_{\mathrm{DLS}}(\boldsymbol{q}^{\dagger})^{\mathrm{T}}\boldsymbol{\lambda}^{+}, \boldsymbol{J}_{\mathrm{DLS}}(\boldsymbol{q}^{\dagger})\dot{\boldsymbol{q}}^{+} = \boldsymbol{0}_{4\times 1}.$$
We then solve the equations for $\boldsymbol{\lambda}^{+} = \begin{bmatrix} \lambda_1^{+} & \lambda_2^{+} & \lambda_3^{+} & \lambda_4^{+} \end{bmatrix}^{\mathrm{T}}$ and $\ddot{\boldsymbol{q}}^{+}$.
2. If $\lambda_2^{+} > 0$ and $\lambda_4^{+} > 0$, then we take $\ddot{\boldsymbol{q}}^{+}$ obtained in 1. as the proper initial acceleration vector and continue the numerical integral. The motion transitions to DLS.
3. If $\lambda_2^{+} > 0$ and $\lambda_4^{+} < 0$, unilateral constraint condition is not satisfied and the motion should transition to SLS. We then break $\boldsymbol{\lambda}^{+}$ and $\ddot{\boldsymbol{q}}^{+}$ obtained in 1., and solve the following equations for $\boldsymbol{\lambda}^{+} \in R^2$ and $\ddot{\boldsymbol{q}}^{+}$.
$$\boldsymbol{M}(\boldsymbol{q}^{\dagger})\ddot{\boldsymbol{q}}^{+} + \boldsymbol{h}(\boldsymbol{q}^{\dagger},\dot{\boldsymbol{q}}^{+},\phi) = \boldsymbol{J}_{\mathrm{SLS}}(\boldsymbol{q}^{\dagger})^{\mathrm{T}}\boldsymbol{\lambda}^{+}, \boldsymbol{J}_{\mathrm{SLS}}(\boldsymbol{q}^{\dagger})\dot{\boldsymbol{q}}^{+} = \boldsymbol{0}_{2\times 1}.$$
4. We take these newly-calculated vectors as the proper initial conditions, and begin the numerical integral.

The measurable period of DLS emerges after impact as shown in Fig. 2 if and only if λ_2^{+}, λ_4^{+}, and λ_{I4} are positive. These three quantities are thus termed as the ***DLS-Indicators*** (DLSIs).

4. Analysis Results of DLSIs

Fig. 3 plots the DLSIs with respect to the leg viscosity, c, in PDW on the slope of ϕ = 0.10 [rad]. The physical parameters were chosen as listed in Table 1. See [2] for the details of the notations. Here, (a) plots λ_{I4} and (b) plots λ_2^{+} and λ_4^{+}. We also plotted their values with different symbols in the case that scuffing of Leg 2 arises; the rear leg quickly extends after takeoff where c is small and the end-point hits the ground. As seen from Fig. 3 (b), λ_4^{+} monotonically decreases as c increases and finally reaches zero where c = 220 [N·s/m]. This implies that unilateral constraint of Leg 2 just after impact does not hold and the stance-leg exchange is then completed instantaneously where $c \geq 220$. λ_{I4} is, however, always positive as shown in Fig. 3 (a). The Jacobian matrix is therefore chosen as $\boldsymbol{J}_I(\boldsymbol{q}^{\dagger}) = \boldsymbol{J}_{\mathrm{DLS}}(\boldsymbol{q}^{\dagger})$ and the impact model is different from the traditional one [1]. On the other hand, λ_2^{+} monotonically decreases as c decreases and finally reaches zero where c = 4.0 [N·s/m]. This implies that bouncing of Leg 1 arises where $c \leq 4.0$.

(a) λ_{I4} [N] (b) λ_2^{+} and λ_4^{+} [N]

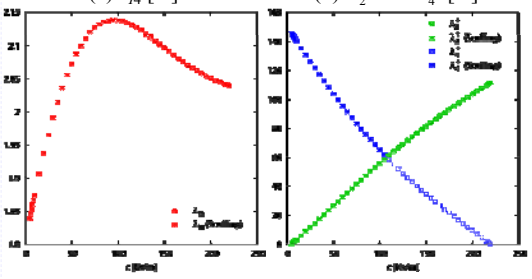

Figure 3: DLSIs with respect c in passive dynamic walking

Table 1: Parameter settings

m_H	10.0	kg
m	1.0	kg
a	0.3	m
L_0	1.0	m
L^*	1.02	m
α	45	deg
k	500	N/m
ϕ	0.1	rad

References

1. T. McGeer, "Passive dynamic walking," *Int. J. of Robotics Research*, Vol. 9, No. 2, pp. 62-82, 1990.
2. F. Asano and J. Kawamoto, "Passive dynamic walking of viscoelastic-legged rimless wheel," *Proc. of the IEEE Int. Conf. on Robotics and Automation*, 2012. (to appear)

Paper ID: 10 **Contact email: fasano@jaist.ac.jp**